Design of dispersive mirrors for ultrafast applications

M. K. Trubetskov

Research Computing Center, Moscow State University, Moscow 119992, Russia

E-mail: trub@srcc.msu.ru

Received November 1, 2009

Different approaches to the design of dispersive mirrors (DMs) for ultrafast applications are considered. High efficiency and good quality of solutions are achieved due to a completely analytical approach to the computations of all DM characteristics and a modern version of the needle optimization technique. Different means to suppress group delay dispersion (GDD) oscillations are demonstrated. Alternatively, design approaches not based on GDD optimization are described, including time-domain design approaches based on direct optimization of pulse energy concentration.

OCIS codes: 320.5520, 310.5696, 310.4165, 310.6805.

doi: 10.3788/COL201008S1.0012.

Since the invention of chirped mirrors[1], compressors based on multilayer mirrors have become more and more popular. Chirped mirrors rely on a multilayer structure with a gradual change in the optical thickness across the structure, resulting in a wavelength-dependent penetration depth of incident radiation[1]. Alternatively, group delay variation may be introduced with resonant structures, implying a wavelength-dependent storage time of incident radiation[2]. In dispersive mirrors (DMs) both effects can coexist, thereby further improving the performance.

In this letter, we consider several possible approaches that will allow one to solve very demanding design problems. All approaches are based on a very efficient needle optimization technique. Firstly, several important aspects of the direct problem solution are considered. They include a completely analytical approach to the computation of all DM spectral characteristics and questions connected with the proper presentation of material dispersive properties. Secondly, we consider a design approach based on the minimization of the merit function, including reflectance and group delay dispersion (GDD). Since this is one of the most popular and widely used approaches, we call it a "classical" approach. Thirdly, we consider a modification of this approach based on the reduction of GDD to phase targets. A special technique permits automatic exclusion of two integration constants from the merit function. Then, we briefly describe the complementary DM pair approach and the double-angle approach, respectively, which are two powerful methods for GDD oscillation suppression. Finally, we consider an alternative approach in the optimization of a special merit function in the time domain. This merit function includes requirements for concentration of pulse energy at some point and maximization of total output pulse energy.

Before considering design problems, it is necessary to define the main spectral characteristics of DMs and introduce a model connecting the optical parameters of a multilayer with its spectral characteristics. Along with reflectance R, DMs are characterized by group delay (GD) and GDD, which are the first and second derivatives of phase on reflection φ with respect to the circular frequency $\omega = 2\pi c/\lambda$, where c is the speed of light and λ is the wavelength:

$$\mathrm{GD} = -\frac{\mathrm{d}\varphi}{\mathrm{d}\omega}, \qquad \mathrm{GDD} = -\frac{\mathrm{d}^2\varphi}{\mathrm{d}\omega^2}. \tag{1}$$

The model of a multilayer system can be obtained directly from Maxwell's equations and methods of calculations of R and φ are well known (see, for example Ref. [3], pp. 2–26). As a result, for multilayers with piece-wise constant refractive index profiles, one can obtain a set of recurrent formulae, including Abelès matrix method[4]. The normal incidence case is considered only in order to make the equations more compact; a generalization on the case of oblique incidence and arbitrary polarization is quite straightforward. Let N be the number of layers, and u_j, v_j $(j = 0, \ldots, N)$ be the values proportional to tangential amplitudes of electric and magnetic fields at layer boundaries, respectively. The boundary between the multilayer and the substrate corresponds to $j = 0$ and the boundary between the multilayer and incident medium corresponds to $j = N$. The matrix method can be written in the form

$$\begin{pmatrix} u_j \\ v_j \end{pmatrix} = M_j \begin{pmatrix} u_{j-1} \\ v_{j-1} \end{pmatrix}, \; M_j = \begin{pmatrix} \cos\phi_j & (i/n)\sin\phi_j \\ i n \sin\phi_j & \cos\phi_j \end{pmatrix},$$
$$j = 1, \ldots N; \quad \begin{pmatrix} u_0 \\ v_0 \end{pmatrix} = \begin{pmatrix} 1 \\ n_s \end{pmatrix}, \tag{2}$$

where $\phi_j = k\, n_j d_j$ are the phase thicknesses of layers with refractive indices n_j and physical thicknesses d_j, $k = 2\pi/\lambda$ is the wave number, and n_s is the substrate refractive index.

Amplitude reflectance r, energy reflectance R, and phase on reflectance φ are expressed through u_N and v_N:

$$r = \frac{n_a u_N - v_N}{n_a u_N + v_N}, \quad R = |r|^2, \quad \varphi = \arg r. \tag{3}$$

One popular and very simple implementation approach for computing GD and GDD is based on finite-difference approximations. For example,

$$\mathrm{GD} \cong -\frac{\varphi(\omega + \Delta\omega/2) - \varphi(\omega - \Delta\omega/2)}{\Delta\omega},$$
$$\mathrm{GDD} \cong -\frac{\varphi(\omega + \Delta\omega) - 2\varphi(\omega) + \varphi(\omega - \Delta\omega)}{\Delta\omega^2}. \tag{4}$$

While the expressions in Eq. (4) have second order of approximations with respect to the small parameter $\Delta\omega$, they are unable to provide the accuracy required for the solution of complicated DM design problems. Attempts to further decrease the value of $\Delta\omega$ in order to improve accuracy lead to fast loss of stability, since round-off computational errors start to reveal in the result and make GD and GDD approximate values very far from the real ones.

The only alternative is to implement a completely analytical and exact approach. Below, we demonstrate only the main idea of this approach. The GD expression can be rewritten as

$$\mathrm{GD} = -\frac{\mathrm{d}\arg\varphi}{\mathrm{d}\omega} = -\frac{1}{c}\mathrm{Im}\frac{\mathrm{d}\ln r}{\mathrm{d}k} = -\frac{1}{c}\mathrm{Im}\left(\frac{1}{r}\frac{\mathrm{d}r}{\mathrm{d}k}\right). \quad (5)$$

We denote the derivatives of u and v with respect to wavenumber k as $\dot{u} = \mathrm{d}u/\mathrm{d}k$ and $\dot{v} = \mathrm{d}v/\mathrm{d}k$. From Eq. (3), it follows that

$$\frac{\mathrm{d}r}{\mathrm{d}k} = \frac{2}{(n_a u_N + v_N)^2} \cdot \left(uv\frac{dn_a}{dk} + n_a v\dot{u}_N - n_a u\dot{v}_N\right). \quad (6)$$

In this expression, n_a is the refractive index of the incident medium. Values of $\dot{u}_N$ and $\dot{v}_N$ are determined, also with the help of a recurrent equation, which can be obtained from Eq. (2) by parameter k differentiation:

$$\begin{pmatrix} \dot{u}_j \\ \dot{v}_j \end{pmatrix} = M_j \begin{pmatrix} \dot{u}_{j-1} \\ \dot{v}_{j-1} \end{pmatrix} + \frac{\mathrm{d}M_j}{\mathrm{d}k}\begin{pmatrix} u_{j-1} \\ v_{j-1} \end{pmatrix},$$

$$j = 1, \ldots, N, \quad \begin{pmatrix} \dot{u}_0 \\ \dot{v}_0 \end{pmatrix} = \begin{pmatrix} 0 \\ \mathrm{d}n_s/\mathrm{d}k \end{pmatrix}. \quad (7)$$

The derivative of characteristic matrix M_j takes the form

$$\frac{\mathrm{d}M_j}{\mathrm{d}k} = \begin{pmatrix} -\sin\phi_j & i/n_j\cos\phi_j \\ in_j\cos\phi_j & -\sin\phi_j \end{pmatrix}\frac{\mathrm{d}\phi_j}{\mathrm{d}k} + \begin{pmatrix} 0 & -i/n_j^2\sin\phi_j \\ i\sin\phi_j & 0 \end{pmatrix}\frac{\mathrm{d}n_j}{\mathrm{d}k}. \quad (8)$$

Equations (2)–(8) describe analytically exact algorithms for the computation of the GD values. By applying one more derivative with respect to k, it is easy to obtain an analytically exact algorithm for the GDD computation. The central part of this algorithm comprises recurrent equation for $\ddot{u}_j = \mathrm{d}^2u_j/\mathrm{d}k^2$ and $\ddot{v}_j = \mathrm{d}^2v_j/\mathrm{d}k^2$, which also includes the values $\dot{u}_j$ and $\dot{v}_j$, determined by the recurrent Eq. (7), and the values u and v, determined by the recurrent Eq. (2). The number of arithmetic operations per layer required for the GD and GDD computations remains constant; thus the described analytical methods are efficient. An analytic approach to the DM design based on a slightly different technique was also reported in Ref. [5], where the authors proposed to use some approximations in order to simplify and accelerate computations.

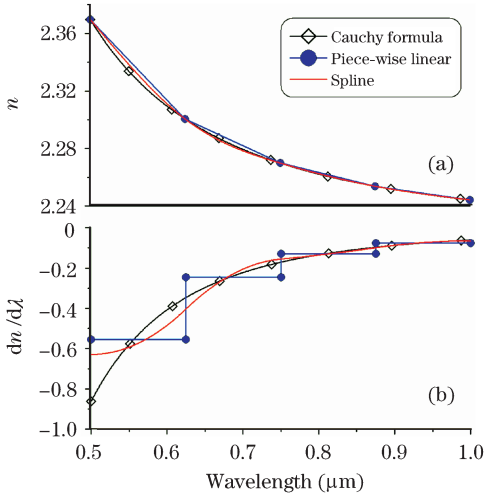

Fig. 1. (a) Refractive indices of Nb_2O_5 represented by the Cauchy formula, piece-wise linear interpolation and interpolating cubic spline; (b) the first derivatives of these refractive index representations are shown at the lower part.

The recurrent Eq. (7) for GD computations includes the first derivatives of the layer materials and substrate refractive indices $\mathrm{d}n_j/\mathrm{d}k$ and $\mathrm{d}n_s/\mathrm{d}k$. The corresponding recurrent equation for the GDD computations includes both the first and second derivatives of these refractive indices. For a presentation of refractive index dispersion dependencies, lookup tables with successive piece-wise linear interpolation are used quite often. In the case of GD and GDD calculation, this approach is not applicable since the first and especially the second derivatives of the refractive index are very far from the expected ones. Figure 1 illustrates the problem of proper refractive index presentation. At the upper part, the refractive index of Nb_2O_5 is represented by the Cauchy's equation:

$$n(\lambda) = n_\infty + A/\lambda^2 + B/\lambda^4, \quad (9)$$

by the piece-wise linear interpolation using five nodes, and by the spline interpolation[6] built with the same five nodes. It is seen that all three representations give a reasonable approximation of the refractive index dispersion. With a growing number of nodes, approximation improves. At the lower part of Fig. 1, the derivatives with respect to λ are represented. The derivative of piece-wise linear approximation is piece-wise constant function and this function is not continuous. Interpolating a spline representation derivative remains continuous, providing a noticeably better approximation.

The situation worsens even further for the case of the GDD calculations, which require second derivatives of the refractive index dispersion. Obviously, the second derivative of the piece-wise linear interpolation gives a sum of Dirac's delta-functions[7], yet the second derivative of the interpolating spline representation still remains a continuous function.

Therefore, in the problems connected with GD/GDD calculations and optimization, it is always necessary to use either analytical expressions for the refractive index dispersions or interpolating spline if analytical expressions are not available.

One of the most widely used modern approaches to the

synthesis problems in multilayer optics is based on the so-called variational formulation. It comprises the introduction of a merit function describing closeness of the current spectral characteristics to the desired characteristics and minimization of this merit function with some combinations of powerful numerical algorithms. In the case of DM design problems, phase requirements are often formulated in terms of pulse GDD, which need to be compensated. Therefore, one of the most widely used merit functions appears as

$$F(\mathbf{X}) = \frac{1}{L}\sum_{m=1}^{L}\left[\left(\frac{R(\lambda_m) - R^{(m)}}{\Delta R^{(m)}}\right)^2 + \left(\frac{\mathrm{GDD}(\lambda_m) - \mathrm{GDD}^{(m)}}{\Delta \mathrm{GDD}^{(m)}}\right)^2\right], \quad (10)$$

where $R(\lambda_m)$ and $\mathrm{GDD}(\lambda_m)$ are theoretical reflectances and GDD values corresponding to the current design, $R^{(m)}$ and $\mathrm{GDD}^{(m)}$ are target values, $\Delta R^{(m)}$ and $\Delta\mathrm{GDD}^{(m)}$ are tolerances, $\lambda_m \quad (m = 1, \ldots, L)$ is the wavelength grid, and $\mathbf{X} = \{d_k\}$ is the vector of layer thicknesses. We call this approach "classical" since it is very widely used in many papers and software packages.

The merit function $F(\mathbf{X})$ typically has numerous numbers of local minima; thus for its optimization, many special approaches are proposed. One of the most efficient approaches is the needle optimization technique (see Ref. [3], Chapter 2), further developed in Refs. [8] and [9] and implemented in the OptiLayer Thin Film software package[10].

For the efficient implementation of the needle optimization technique, it is necessary to obtain analytically accurate equations and algorithms for the calculation of a gradient of the merit function and the perturbation function used in the needle optimization procedure. Optionally, analytically accurate equations for the Hesse matrix may be necessary for the use of the second-order optimization methods. The derivation of the corresponding equations was performed in the same way as described in Eqs. (5)–(8). It is based on the corresponding recurrent formulae for conjugated problems[3,11].

The $\mathrm{GDD}^{(m)}$ values in Eq. (10) are often specified in the following way. It is convenient to express the target GDD in terms of pulse GDD that needs to be compensated. Usually, the pulse characteristics are given at some wavelength $\lambda_0 = 2\pi c/\omega_0$ positioned at the center of its spectral distribution. Values of $\mathrm{GDD}^{(m)}$ at different wavelengths can be computed using several terms of the Taylor series. For example,

$$\mathrm{GDD}(\omega) = \mathrm{GDD} + \mathrm{TOD}(\omega - \omega_0) + 0.5\mathrm{FOD}(\omega - \omega_0)^2. \quad (11)$$

Consider an example of an application of the "classical" approach. In this example and all other examples of the letter, we consider a Suprasil substrate and SiO_2 and Nb_2O_5 as layer materials. All materials are nonabsorbing; refractive indices are given by Eq. (9), with coefficients shown in Table 1 (wavelength should be expressed in microns).

The wavelength range will be from $\lambda_{\min} = 550$ nm to $\lambda_{\max} = 1100$ nm, therefore, we consider a one-octave DM design problem. We consider a wavelength grid consisting of 1024 points distributed according to the equation:

$$\lambda_m = \lambda_{\min} r^{j-1}, r = \exp\left(\frac{\ln(\lambda_{\max}/\lambda_{\min})}{L-1}\right), \quad j = 1, \ldots, L. \quad (12)$$

This distribution provides higher density of wavelength points in a short wavelength region.

The target reflectances $R^{(m)}$ are 100%. The $\mathrm{GDD}^{(m)}$ values are given by Eq. (11) with parameters GDD = -40 fs^2, TOD = -10 fs^3, and FOD = 0.0 fs^4 at $\lambda_0 = 790$ nm. In this example and below, the angle of incidence is 7° for the p-polarized light.

We use a 70-layer mirror with a central wavelength of 790 nm and linearly decreasing thicknesses from 1.4 QWOT (quater-wave optical thickness) (substrate side) to 0.6 QWOT (air side) as a starting design to accelerate

Table 1. Cauchy Formula Coefficients for the Substrate and Layer Materials

	n_∞	A	B
Suprasil	1.4433	4.05996E-3	6.94818E-6
SiO_2	1.4653	0.0	4.71080E-4
Nb_2O_5	2.2185	2.18268E-2	0.0040

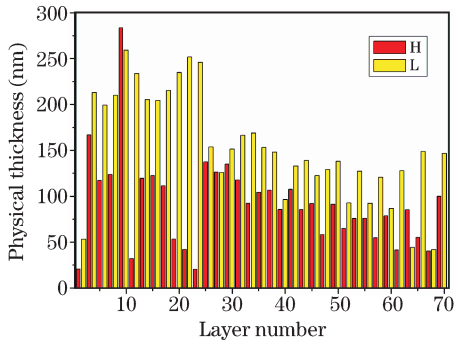

Fig. 2. Layer thicknesses of a 70-layer DM obtained with the "classical" approach.

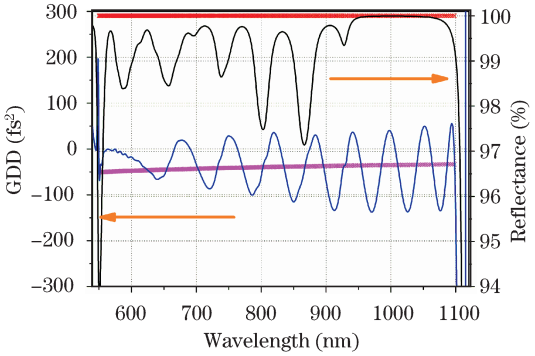

Fig. 3. GDD (left axis) and reflectance (right axis) of a 70-layer DM obtained with the "classical" approach. Crosses designate the specified target values.

computations. Here dimensionless QWOT units are related to the central wavelength of the mirror. One of the possible multiple solutions to the problem is presented in Fig. 2. This DM provides reflectance and GDD, as shown in Fig. 3.

It is well known that for broadband high-reflection DM designs, oscillations of GDD in this band are inevitable[12−14]. A large level of GDD oscillations can destroy the shape of output pulses, especially when oscillations are not "regular", that is, when the average level of obtained GDD deviates significantly from target values, or shapes of adjacent oscillations are significantly different. From this point of view, the solution obtained with the "classical" approach Fig. 3 is not optimal, one can expect a significant degradation of the output pulse characteristics.

In order to improve the quality of solutions and extend the set of design problems, a new method of phase optimization with floating constants is proposed. Any given dependence GDD(ω) can be integrated twice and this is converted to the phase target:

$$\hat{\varphi}(\omega) = \int_{\omega_0}^{\omega} \mathrm{d}\omega_1 \int_{\omega_0}^{\omega_1} \mathrm{GDD}(\omega_2)\, \mathrm{d}\omega_2 + C_1\omega + C_2, \qquad (13)$$

where C_1 and C_2 are arbitrary integration constants. Instead of the merit function Eq. (10), it is natural to consider another merit function with a phase term,

$$F(\mathbf{X}, C_1, C_2) = \frac{1}{L}\sum_{m=1}^{L}\left[\left(\frac{R(\lambda_m) - R^{(m)}}{\Delta R^{(m)}}\right)^2 + \left(\frac{\varphi(\lambda_m) - \varphi^{(m)}}{\Delta\varphi^{(m)}}\right)^2\right], \qquad (14)$$

where phase targets $\phi^{(m)} = \hat{\varphi}(\omega_m)$, and therefore include constants C_1 and C_2.

Optimization of the merit function Eq. (14) was first proposed in Ref. [12]; however, in this work, integration constants were chosen by the trial-and-error method. A much more advanced approach is based on an automated exclusion of these constants from the merit function Eq. (14). It is easy to see that $F(\mathbf{X}, C_1, C_2)$ depends on the variables C_1 and C_2 quadratically, therefore, for any vector of thicknesses $\mathbf{X}$, there exists an unique combination of C_1^* and C_2^*, providing a minimum value of $F(\mathbf{X}, C_1, C_2)$. The values C_1^* and C_2^* are determined analytically as a solution of a system of linear equations $\partial F(\mathbf{X}, C_1, C_2)/\partial C_1 = 0$, $\partial F(\mathbf{X}, C_1, C_2)/\partial C_2 = 0$. This allows us to exclude these constants from the optimization problem and to reduce the optimization problem to the form that allows us to apply the needle optimization technique. Let us call this approach "optimization with floating constants".

Implementation of this approach requires taking into account additional terms appearing in the expressions for the gradient of the merit function Eq. (14) and perturbation function used in the needle optimization. Also,

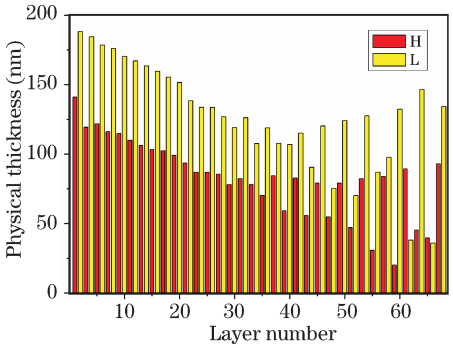

Fig. 4. Layer thicknesses of a 68-layer DM obtained with phase optimization approach.

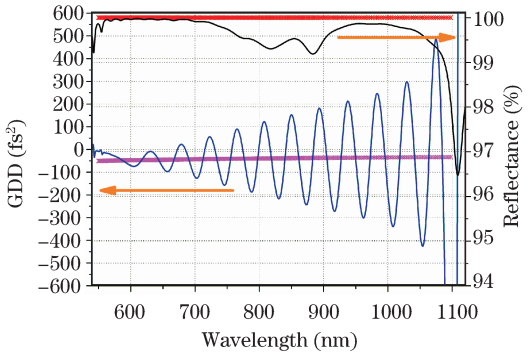

Fig. 5. GDD (left axis) and reflectance (right axis) of a 68-layer DM obtained with phase optimization approach. Red crosses designate specified target reflectances. Magenta crosses designate GDD target values used in Eq. (13) to obtain phase target.

it is necessary to take into account the problem of phase unwrapping. The function $\varphi = \arg r$ (Eq. (3)) is multivalued. Correct implementation of the described method requires computation of the same branch of this function for any wavelength in the considered region.

Application of the phase optimization approach to the problem considered in the previous part gives the solution shown in Fig. 4. Computations are significantly faster in this case (the same starting design is used) because complicated GDD computations are not needed; also, the merit function Eq. (14) is more convenient for optimization methods because it has a simpler structure of relief.

The obtained reflectance and GDD are shown in Fig. 5. In spite of the fact that only phases are present in the merit function Eq. (14), the obtained GDD curve oscillates very closely around the initial GDD target (magenta crosses). The amplitude of oscillation grows when wavelength increases; the oscillation pattern has a rather "regular" character. We will see that a time-domain approach gives similar structures of DM designs.

A powerful method for suppression of the GDD oscillation is based on using complimentary pairs of DMs. In Ref. [15], a pair of 1.5-octave DMs was demonstrated both theoretically and experimentally. Here, we limit ourselves to the same one-octave design problem in order to be able to compare various design approaches. We define the reflectance and GDD of a DM pair using the equation

$$R_p = (R_1 R_2)^{1/2}, \ \mathrm{GDD}_p = (\mathrm{GDD}_1 + \mathrm{GDD}_2)/2, \qquad (15)$$

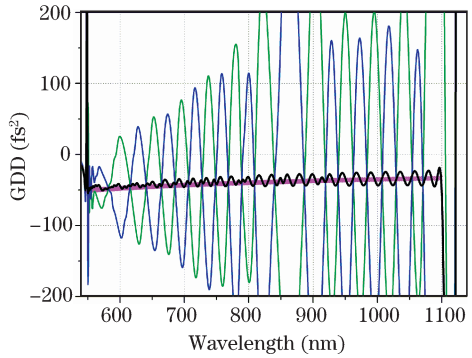

Fig. 6. GDD of a DM pair (black curve), GDD of the first DM (blue curve), and GDD of the second DM (green curve). Target GDD values are shown by magenta crosses.

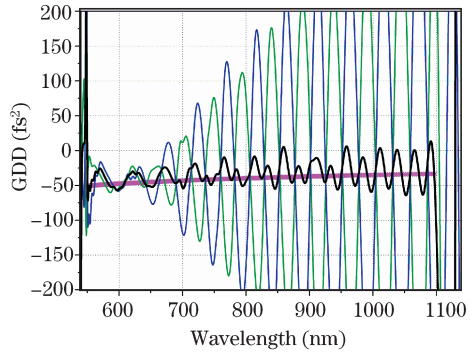

Fig. 7. The resulting GDD of a DM pair (black curve) working at two incident angles, GDD of the first DM (blue curve) working at 7°, and GDD of the second DM (green curve) working at 22°. Target GDD values are shown by magenta crosses.

and use these values in the merit function Eq. (10). In the case of a DM pair vector of parameters, $\mathbf{X}$ consists of both design thicknesses. Generalization of the needle optimization technique for this case requires corresponding modifications for gradient and perturbation function computations. During the needle step, it is necessary to consider both designs, consequently looking for the best position for the insertion of a new layer.

In Fig. 6, the resulting GDD_p of the designed pair (72 and 70 layer mirrors) is shown with black line; the level of its oscillations is very low compared to a single mirror. Suppression of oscillations was achieved due to the fact that oscillations of the mirrors in the pair are in antiphase. Manufacturing complementary mirror pairs is a challenging task[15]. Special procedures should be applied in order to find a more robust solution. Mirrors in the pair are produced in different deposition runs; in order to achieve a high level of oscillation suppression both runs should perfectly match.

It is possible to suppress GDD oscillations using mirrors deposited in a single run. The effect of suppression is achieved when these mirrors work at different angles of incidence[16], due to a shift of spectral characteristics with changing incidence angle. From the mathematical and implementation point of view, this problem is rather close to the complimentary pair design. An important difference for the double angle approach is the definition of the parameter vector $\mathbf{X}$, which now includes thicknesses of a single mirror.

Figure 7 demonstrates a good suppression of GDD oscillations with double angle approach, achieved in the same one-octave DM design problem. Mirrors of the pair are working at 7° and 22° angles of incidence; the mirror consists of 80 layers. Of course, the suppression in the double angle case is less than that in the case of the complimentary pair, but all mirrors of a compressor are deposited in the same deposition run and therefore automatically match. Therefore, the double angle approach allows us to design more practical DMs with better stability with respect to manufacturing errors.

An interesting and promising alternative to the DM design in spectral domain considered above is the time-domain design approach[17−19]. If an intensity spectrum $I_{\mathrm{in}}(\omega)$ and a phase $\varphi_{\mathrm{in}}(\omega)$ of an input pulse are known, one can compute the corresponding output pulse characteristics. If the pulse exhibits n bounces inside a compressor with the same mirrors, the output pulse $\hat{A}_{\mathrm{out}}(\omega)$ can be represented as

$$\hat{A}_{\mathrm{out}}(\omega) = [r(\omega)]^n \hat{A}_{\mathrm{in}}(\omega),$$
$$\hat{A}_{\mathrm{in}}(\omega) = I_{\mathrm{in}}(\omega)\ \exp(\mathrm{i}\phi_{\mathrm{in}}(\omega)), \qquad (16)$$

where $r(\omega)$ is the amplitude reflectance of the mirror. The temporal shape of the output pulse is obtained with the help of Fourier transform; for numerical implementation fast Fourier transform algorithms should be used[20]. The main idea of the time-domain approach comprises the optimization of a special merit function describing concentration of pulse energy at some temporal point t_0 and also includes the requirement for pulse energy maximization[17]:

$$\Phi = (E_p)^{-q} \int_{-\infty}^{+\infty} (t - t_0)^2 \, |A_{\mathrm{out}}(t)|^p \, \mathrm{d}t,$$
$$t_0 = (E_p)^{-1} \int_{-\infty}^{+\infty} t \, |A_{\mathrm{out}}(t)|^p \mathrm{d}t,$$
$$E_p = \int_{-\infty}^{+\infty} |A_{\mathrm{out}}(t)|^p \mathrm{d}t, \quad q \geq 1. \qquad (17)$$

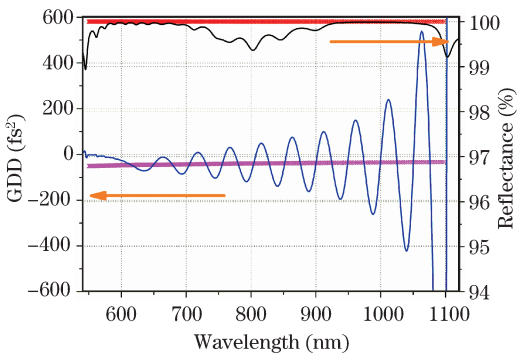

Fig. 8. GDD (left axis) and reflectance (right axis) of a 68-layer DM obtained with the time-domain approach. Red crosses designate specified target reflectances. Magenta crosses designate GDD of the input pulse with the opposite sign.

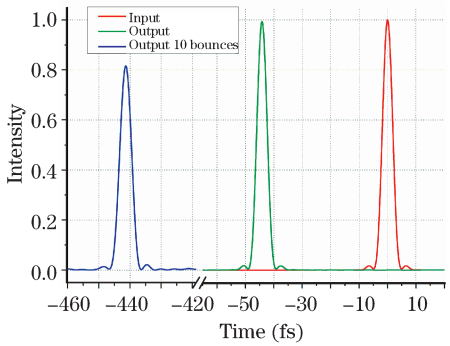

Fig. 9. Bandwidth limited input pulse envelope (red curve), the envelope of the output pulse after one reflection (green curve), and the envelope of the output pulse (blue curve) after 10 bounces for the 68-layer DM obtained by time-domain needle optimization.

The introduction of two parameters p and q gives a high level of flexibility.

Numerical tests and some additional considerations[17] allow us to select $p = 4$ and $q = 3$, giving the best design results.

To illustrate the time-domain optimization approach we considered a similar design problem of the compression of a pulse with super-Gaussian spectrum intensity centered at 790 nm and half-width of 500 THz; the GDD of this pulse was specified by Eq. (11), with GDD = 40 fs^2, TOD = 10 fs^3, and FOD = 0.0 fs^4. A special version of the needle optimization technique based on the optimization of the merit function Eq. (17) allows us to obtain a 68-layer DM with reflectance and GDD, as shown in Fig. 8. It is interesting to note that the GDD spectral dependence looks quite similar to the GDD spectral dependence obtained with the phase optimization approach (see Fig. 5).

The time-domain approach allows us to investigate the shapes of the envelope of output pulses (Fig. 9). Even after 10 bounces, the intensity of the output pulse is still higher than 80% of the input pulse. Additional information on comparison of mirrors obtained with the time-domain approach and "classical" approach can be found in Ref. [19]. The time-domain approach is especially efficient and useful when reliable information concerning the characteristics of pulses to be compressed is known.

In conclusion, several DM design approaches having high efficiency and different areas of application were described and demonstrated. All approaches were implemented either directly using the OptiLayer Thin Film software[10] or as special plug-in extension modules. Some approaches can be combined; for example, the time-domain optimization of complimentary DM pairs is available. Having several highly efficient DM design approaches allows a researcher to select the approach best suited to his requirements and to solve the most challenging design problems.

References

1. R. Szipöcs, K. Ferencz, C. Spielmann, and F. Krausz, Opt. Lett. **19,** 201 (1994).
2. R. Szipöcs, A. Koházi-Kis, S. Lako, P. Apai, A. P. Kovács, G. DeBell, L. Mott, A. W. Louderback, A. V. Tikhonravov, and M. K. Trubetskov, Appl. Phys. B **70,** S51 (2000).
3. Sh. Furman and A. V. Tikhonravov, *Basics of Optics of Multilayer Systems* (Edition Frontieres, Gif-sur-Yvette, 1992), see also http://www.optilayer.com.
4. F. Abelès, Ann. de Physique **5,** 706 (1950).
5. J. R. Birge and F. X. Kärtner, Appl. Opt. **46,** 2656 (2007).
6. J. H. Ahlberg, E. N. Nilson, and J. L. Walsh, *The Theory of Splines and Their Applications* (Academic Press, New York, 1967).
7. I. M. Gel'fand and G. E. Shilov, *Generalized Functions* (Academic Press, New York, 1966).
8. A. V. Tikhonravov, M. K. Trubetskov, and G. W. DeBell, Appl. Opt. **35,** 5493 (1996).
9. A. V. Tikhonravov, M. K. Trubetskov, and G. W. DeBell, Appl. Opt. **46,** 704 (2007).
10. A. V. Tikhonravov and M. K. Trubetskov, "OptiLayer Thin Film Software" http://www.optilayer.com.
11. A. N. Tikhonov, A. V. Tikhonravov, and M. K. Trubetskov, J. Comput. Math. Math. Phys. **33,** 1339 (1993).
12. A. V. Tikhonravov, M. K. Trubetskov, and A. A. Tikhonravov, OSA Technical Digest Series 9 (*Optical Interference Coatings*) *Washington DC, USA* (1998).
13. A. V. Tikhonravov, M. K. Trubetskov, U. Keller, and N. Matuschek, Proc. SPIE **3738,** 221 (1999).
14. G. Steinmeyer, Appl. Opt. **45,** 1484 (2006).
15. V. Pervak, A. V. Tikhonravov, M. K. Trubetskov, S. Naumov, F. Krausz, and A. Apolonski, Appl. Phys. B. **87,** 5 (2007).
16. V. Pervak, I. Ahmad, M. K. Trubetskov, A. V. Tikhonravov, and F. Krausz, Opt. Express **17,** 7943 (2009).
17. P. Dombi, V. S. Yakovlev, K. O'Keeffe, T. Fuji, M. Lezius, and G. Tempea, Opt. Express **13,** 10888 (2005).
18. M. K. Trubetskov, A. V. Tikhonravov, and V. Pervak, Opt. Express **16,** 20637 (2008).
19. V. Pervak, I. Ahmad, J. Fulop, M. K. Trubetskov, and A. V. Tikhonravov, Opt. Express **17,** 2207 (2009).
20. J. W. Cooley and J. W. Tukey, Math. Comput. **19,** 297 (1965).